

Elastic Scattering of 600-MeV Protons from H, D, ^3He , and ^4He

E. T. Boschitz,* W. K. Roberts, and J. S. Vincent

National Aeronautics and Space Administration, Lewis Research Center, Cleveland, Ohio 44135

and

M. Blecher† and K. Gotow†

Virginia Polytechnic Institute and State University, Blacksburg, Virginia 24061

and

P. C. Gugelot

University of Virginia, Charlottesville, Virginia

and

C. F. Perdrisat and L. W. Swenson‡

College of William and Mary, Williamsburg, Virginia

and

J. R. Priest

Miami University, Oxford, Ohio

(Received 16 March 1972)

The elastic scattering of 600-MeV protons from light nuclei has been studied at the National Aeronautics Space Administration Space Radiation Effects Laboratory (SREL) synchrocyclotron. Differential cross sections have been obtained for the scattering of protons from hydrogen, deuterium, helium-3, and helium-4. Polarization was measured for deuterium and ^4He nuclei. The p - p cross-section data are in excellent agreement with the predictions from the Livermore phase shifts. Small-angle p -D, p - ^3He elastic scattering data are compared with calculations based on the multiple-scattering theories of Watson and Glauber.

INTRODUCTION

During the past few years there has been a growing interest in probing the nucleus with intermediate-energy hadrons. This interest is based on the fact that the scattering of particles for which the wavelength is comparable or less than the internucleon spacings may yield information which is not forthcoming from experiments at lower energies, e.g. one might learn about the behavior of individual nucleons within the nucleus.

A number of experiments have been reported on the differential and total cross section in hadron-nucleus scattering.¹⁻⁵ Analyses of these experiments have been made using the multiple-scattering theories of Glauber⁶ and Watson⁷ and the optical potential model of Kerman, McManus, and Thaler.⁸ Pion scattering cross sections for ^{16}O and ^{12}C near the 3,3 resonance can be well described⁹⁻¹¹ in the Glauber approximation but the success of the model at this low energy and for large scattering angles is not understood. Both multiple-scattering theory¹¹ and optical models^{12, 13} have been used to predict differential cross sections in p - ^4He and p - ^{16}O scattering at high ener-

gies. The primary theoretical interest here was to detect nucleon-nucleon short-range correlations. The results of these calculations¹³ indicate the possibility of pair correlations but definitive statements are contingent upon better knowledge of nucleon-nucleon scattering amplitudes.

In view of the considerable theoretical interest and the efforts being made in interpreting hadron-nucleus scattering we have attempted to provide more complete data for proton scattering from the lightest nuclei. In the present work we have measured the elastic differential cross section and polarization for 600-MeV proton scattering from H, D, ^3He , and ^4He .

EXPERIMENTAL PROCEDURE

A. Proton Beam and Monitoring

The experimental arrangement is shown in Fig. 1. The external proton beam of the Space Radiation Effects Laboratory (SREL) 600-MeV proton synchrocyclotron was brought to a focus on the target by the beam transport system. The beam spot at the target position was about 2.5 cm high and 1.25 cm wide with a divergence of $\pm\frac{1}{2}^\circ$ for both polarized

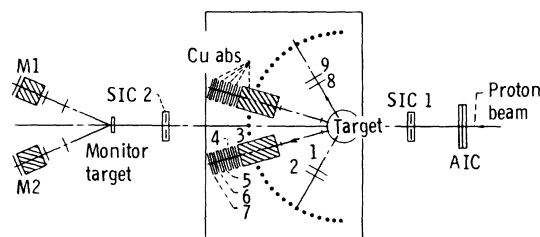


FIG. 1. Experimental arrangement.

and unpolarized beams. Two split ion chambers (SIC 1 and SIC 2) determined the beam centroid at two positions, and gave the reference line for the experimental setup. The scattering table was aligned with respect to this line and the zero of the scattering angle was determined to an accuracy of $\pm 0.03^\circ$. The sum and difference of the current outputs from each split ion chamber were continuously monitored on a strip chart recorder. The relative beam intensity was monitored with an argon-filled ion chamber (AIC) and with a pair of counter telescopes, M1 and M2, viewing an auxiliary target. These telescopes provided the correct normalization as long as all the beam passed through the main target. When the main target was smaller than the beam, an additional monitor telescope viewing only the main target was mounted above the scattering table at about 45° to the scattering plane. These monitor counters were cali-

brated in separate runs where their accumulated counts were compared with the activity produced in a carbon target. The well-known $^{12}\text{C}(p, pn)^{11}\text{C}$ cross section¹⁴ (30.5 ± 0.6 mb at 600 MeV) was used. The usable maximum intensity of the unpolarized beam was initially limited to $\sim 2 \times 10^7$ protons/sec because of a small duty cycle factor (2 to 6×10^{-4}) of the regenerative extraction system. During the latter phases of the experiments, however, the beam was extracted stochastically such that about 10^{10} protons/sec were ejected after the initial burst. All counters were then electronically gated to obscure this burst so that an effective beam of 5×10^9 protons/sec gave less than 10% random coincidences.

The polarized proton beam was produced by scattering the cyclotron beam from an internal carbon block. Its azimuthal position was such that protons scattered at $9 \pm 1^\circ$ entered the beam transport system. The maximum intensity of the polarized proton beam was about 3×10^7 protons/sec. To determine the beam polarization, four separate double-scattering experiments were performed and the measured asymmetries were compared with polarizations of Cheng *et al.*¹⁵ and Azhgirei *et al.*¹⁶ Elastic scattering from carbon at 6, 8, and 10° lab yielded asymmetries of 0.119 ± 0.002 , 0.146 ± 0.002 , and 0.148 ± 0.003 , respectively. At 15° lab, the asymmetry from p - p scattering was 0.195 ± 0.017 . The analyzing powers obtained from

TABLE I. Counter sizes and experimental geometries.

Reaction	Angular range covered, $\theta_{p, \text{lab}}$ (deg)	Frontal dimensions of counters (horizontal and vertical) and target to counter distance ^a		Distance between counter 8 and target (cm)
		Counter 1	Counter 2	
p - p (CH_2 target)	All angles	2.54×7.62 cm at 30.5 cm	1.27×5.08 cm at 114 cm	30.5
p - p (gas target)	45	0.635×10.16 cm at 30.5 cm	1.27×5.08 cm at 114 cm	30.5
p -D and \bar{p} -D	10-12	2.54×7.62 cm at 114 cm	1.27×5.08 cm at 175 cm	25.4
	15-27	2.54×7.62 cm at 6 cm	1.27×5.08 cm at 114 cm	38
	30-32	2.54×7.62 cm at 50.8 cm	1.27×5.08 cm at 67.3 cm	25.4
	35-40	2.54×7.62 cm at 50.8 cm	1.27×5.08 cm at 67.3 cm	38
	45-60	2.54×7.62 cm at 50.8 cm	1.27×5.08 cm at 67.3 cm	58.5
	60-150 ^b	2.54×7.62 cm at 61 cm	1.27×5.08 cm at 114 cm	30.5
p - ^3He	17-26.5	0.635×10.16 cm at 30.5 cm	2.54×7.62 cm at 114 cm	30.5
	20-28	0.635×10.16 cm at 30.5 cm	1.27×5.08 cm at 61 cm	25.4
	28-45	0.635×10.16 cm at 30.5 cm	2.54×7.62 cm at 61 cm	25.4
p - ^4He and \bar{p} - ^4He	4-18	No counter	1.27×5.08 cm at 114 cm	No associate counter ↓
	15-32	0.635×10.16 cm at 30.5 cm	1.27×5.08 cm at 175 cm	
	19-32	0.635×10.16 cm at 30.5 cm	1.27×5.08 cm at 114 cm	
	19-60	0.635×10.16 cm at 61 cm	1.27×5.08 cm at 175 cm	

^a Scintillators 3-9 were 12.7 cm wide and 17.8 cm high. All scintillators were 0.635 cm thick.^b Deuteron defines solid angles.

these measurements were 0.325 ± 0.015 , 0.384 ± 0.015 , and 0.410 ± 0.015 for the respective angles with carbon and 0.488 ± 0.025 for hydrogen. The beam polarization deduced was 0.369 ± 0.015 (^{12}C) and 0.400 ± 0.040 (H).

The beam energy was determined by measuring the mean range in copper of protons scattered from carbon and hydrogen. The proton energy equivalent to this range was taken from the tabulation of Janni.¹⁷ The energies were 594 and 554 MeV for the unpolarized and polarized proton beams, respectively. Stochastic extraction caused a slight reduction in energy, viz. 580 and 544 MeV, respectively. The beam energy spread amounted to 10 MeV [full width at half maximum (FWHM)] for the unpolarized and 30 MeV (FWHM) for the polarized beam, respectively.

B. Targets

The hydrogen targets used in the p - p scattering measurements were thin polyethylene sheets ranging in thickness from 0.025 to 1.28 cm. Subtraction of events due to scattering from ^{12}C in the CH_2 was performed using scattering data from pure carbon targets having equivalent numbers of carbon nuclei.

Deuterated polyethylene targets were used in the p -D scattering measurements. The targets contained less than 2% ^1H as determined by mass-spectroscopic analysis.

Gaseous ^3He was contained in 15-cm-diam by 10-cm-high cylinders. For angles where the recoiling ^3He energy was low, the target walls were 0.0025-cm-thick Havar foil and the pressure was 3 atm absolute. For larger angles the wall thickness was increased to 0.0075 cm and the gas pressure to 11 atm.

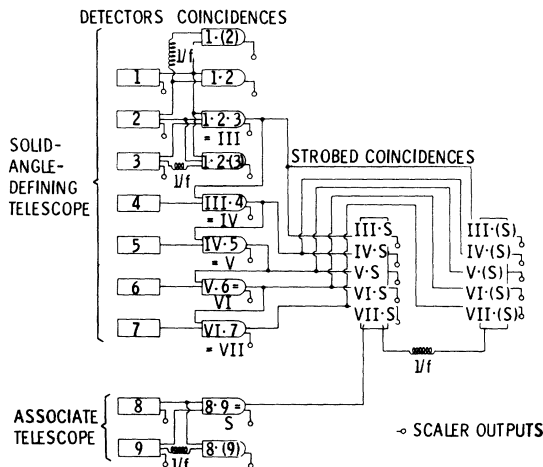


FIG. 2. Electronic logic.

The ^4He target was loaned to us from the Brookhaven National Laboratory.¹⁸ Liquid helium was contained in a right circular cylinder of 0.025-cm Mylar film 12.5 cm high and 10 cm in diameter.

C. Detectors

Figure 1 shows a differential range telescope consisting of seven detectors. A large block of copper was placed between detectors 2 and 3 as the main energy degrader. Thin copper plates were sandwiched between detectors 3 to 7 to scan the end of the range curve. These detectors were large enough to keep counting losses due to multiple scattering smaller than 1%. Each detector in the telescopes consisted of a plastic scintillator, a Lucite light guide, and a photomultiplier assembly. In the case of a liquid or gaseous target, scintillators 1 and 2 jointly defined the scattering volume and the solid angle. For solid targets only scintillator 2 was used to define the solid angle, while scintillator 1 provided an additional coincidence requirement greatly reducing the number of random events.

In the case of p - p , p -D, and p - ^3He scattering the recoiling target nuclei were detected in an associated particle telescope to ensure elastic scattering. The dimensions of counters and the experimental geometries are contained in Table I. The range telescope (counters 1-7) and the associate telescope (counters 8 and 9) provided the necessary coincidence requirements. Only one such set of telescopes was used for the cross-section measurements, while for the polarization study two

TABLE II. p - p differential cross section at 582 MeV.

Proton center-of-mass scattering angle $\theta_{p, \text{c.m.}}$ (deg)	Center-of-mass differential cross section and error, $\left(\frac{d\sigma}{d\Omega}\right)_{\text{c.m.}} \pm \Delta \left(\frac{d\sigma}{d\Omega}\right)_{\text{c.m.}}$ (mb/sr)
15	5.98 ± 0.25
20	5.91 ± 0.18
27.4	5.45 ± 0.16
27.4 ^a	5.78 ± 0.21
30	5.13 ± 0.10
30	5.40 ± 0.09
40	4.55 ± 0.08
50	3.95 ± 0.09
60	3.47 ± 0.06
70	2.72 ± 0.05
80	2.80 ± 0.06
90	2.58 ± 0.05
90 ^b	2.53 ± 0.07

^a Measured with time-of-flight system.

^b Measured with a gas target.

identical sets were used. The arms for the range telescopes were positioned to an accuracy of $\pm 0.01^\circ$, the arm of the associate telescope to $\pm 0.5^\circ$.

To determine the telescope efficiency, absorption curves were obtained at five beam energies (580, 493, 413, and 288 MeV) by placing a copper wedge of variable thickness between counters 2 and 3 and recording the ratio of coincidences $1 \cdot 2 \cdot 3 / 1 \cdot 2$ vs absorber thickness. The ratio of $1 \cdot 2 \cdot 3 / 1 \cdot 2$ for any absorber thickness was defined as the telescope efficiency at that proton energy. Each efficiency curve was plotted as a function of reduced range (reduced range is defined as the thickness of absorber in the telescope divided by the mean range of the proton).

In addition to these measurements, a Monte Carlo calculation for the penetration of the protons

through a copper slab was performed, using known reaction cross sections in the energy range 10 to 600 MeV and making reasonable assumptions for the angular distribution and energy spectra of the reaction products. 10% agreement between the calculated and the experimentally observed absorption curve was obtained.

D. Electronic Logic

The electronic logic for the elastic scattering and polarization measurement is shown schematically in Fig. 2. In the defining telescope twofold, threefold, fourfold, fivefold, sixfold, and sevenfold coincidences were formed multiplicatively, but only the twofold and threefold random coincidence rates were determined. Fourfold and higher-order random coincidence rates were found to be negligible at the selected beam levels. In the associate telescope, a double coincidence (8 · 9) was made when the range of the incident particle was sufficiently long. The associate telescope signal was used to gate the various coincidence outputs from the proton telescope by means of a strobed coincidence unit. These signals are labeled III · S, IV · S, etc. Random strobed coincidences III · (S), IV · (S), etc. were formed in a second strobe unit by delaying the strobing signal by 58 nsec, the microscopic beam period.

E. Specific Experimental Techniques

p-p

The proton-proton differential cross section was determined using the associated-particle method without range requirements on the recoiling protons. The cross section at 90° in the center of

TABLE III. *p*-D differential cross section at 582 MeV.

Proton center-of-mass scattering angle, $\theta_{p, \text{c.m.}}$ (deg)	Center-of-mass differential cross section and error, $\left(\frac{d\sigma}{d\Omega}\right)_{\text{c.m.}} \pm \Delta \left(\frac{d\sigma}{d\Omega}\right)_{\text{c.m.}}$ (mb/sr)
16.9	11.9 ± 1.9
20.3	7.7 ± 0.6
20.3 ^a	6.9 ± 0.6
25.3	3.7 ± 0.6
28.6	3.1 ± 0.5
33.6	1.24 ± 0.10
36.8	0.82 ± 0.07
41.7	0.38 ± 0.02
44.9	0.27 ± 0.02
49.6	0.15 ± 0.01
52.8	0.11 ± 0.01
57.4	0.091 ± 0.005
60.5	0.081 ± 0.005
65.0	0.091 ± 0.005
72.7	0.083 ± 0.005
79.5	0.071 ± 0.003
86.2	0.055 ± 0.003
92.7	0.045 ± 0.002
99.0	0.039 ± 0.005
104.9	0.028 ± 0.002
110.6	0.023 ± 0.002
116.0	0.022 ± 0.002
126.0	0.024 ± 0.003
134.8	0.037 ± 0.003
142.5	0.071 ± 0.007
149.5	0.117 ± 0.018
154.0 ^a	0.121 ± 0.009
155.6	0.172 ± 0.008
161.2	0.168 ± 0.007
166.2	0.172 ± 0.026

^a Measured with time-of-flight system.

TABLE IV. *p*-D polarization at 544 MeV.

Center-of-mass scattering angle, $\theta_{\text{c.m.}}$ (deg)	Polarization and error, $P \pm \Delta P$
16.8	0.484 ± 0.091
25.1	0.535 ± 0.028
33.3	0.482 ± 0.035
41.3	0.267 ± 0.102
49.2	-0.051 ± 0.068
56.9	-0.304 ± 0.056
64.5	-0.149 ± 0.075
71.8	-0.135 ± 0.105
77.5	0.025 ± 0.070
92.2	-0.058 ± 0.077
104.4	-0.061 ± 0.084
116.0	0.010 ± 0.140
125.5	-0.074 ± 0.115

mass was measured with both a hydrogen-gas target of 65 atm pressure and a CH₂ target. The cross sections obtained by the two methods agreed within statistics. Good agreement was also obtained at 12° using magnetic analysis and a time-of-flight system. This system consisted of three detectors along a 7-m flight path through a 22° bending magnet. The time and spatial resolution was sufficient to separate elastic scattering events from background.

p-D

The associate particle technique was also used in the *p*-D scattering. To determine the contribution due to deuteron breakup data were accumulated with and without an absorber in the deuteron telescope. Measurements of the angular correlation around the elastic kinematic angle verified this correction for breakup events. The yield of scattered protons was obtained from the difference of CD₂ and C measurements.

As an additional test, the magnetic spectrometer and time-of-flight system were used to separate deuterons from breakup protons. The cross section was measured at $\theta_p = 12^\circ$ lab and the values which were found (σ spectrometer = 19.2 ± 1.7 mb/sr) agreed very well with the cross sections determined by the coincidence range method (σ range = 21.5 ± 1.7 mb/sr).

For the *p*-D polarization measurement all four telescopes shown in Fig. 1 were used. During the experiment corresponding pairs of telescopes were

TABLE V. *p*-³He differential cross section at 582 MeV.

Proton center-of-mass scattering, angle, $\theta_p, \text{c.m.}$ (deg)	cross section and error, $\left(\frac{d\sigma}{d\Omega}\right)_{\text{c.m.}} \pm \Delta \left(\frac{d\sigma}{d\Omega}\right)_{\text{c.m.}}$ (mb/sr)
24.7	3.40 ± 0.30
27.6	1.52 ± 0.18
29.0	0.65 ± 0.13
32.5	0.74 ± 0.05
33.4	0.211 ± 0.021
34.7	0.159 ± 0.050
36.1	0.061 ± 0.005
38.2	0.039 ± 0.005
40.3	0.038 ± 0.004
43.1	0.038 ± 0.004
47.2	0.043 ± 0.003
49.9	0.044 ± 0.003
52.6	0.036 ± 0.004
56.6	0.026 ± 0.003
59.3	0.023 ± 0.003
63.2	0.027 ± 0.014

interchanged several times at each angle to eliminate some of the instrumental asymmetries.

p-³He

The *p*-³He differential cross section was measured in a manner similar to the *p*-D scattering. However, ³He attenuation curves were mapped at several angles in order to estimate the contribution of nonelastic events due to the breakup of ³He. From the shape of the attenuation curves, it was

TABLE VI. *p*-⁴He elastic cross sections at 587 MeV.

Proton center-of-mass scattering angle, $\theta_p, \text{c.m.}$ (deg)	Center-of-mass differential cross section and error, $\left(\frac{d\sigma}{d\Omega}\right)_{\text{c.m.}} \pm \Delta \left(\frac{d\sigma}{d\Omega}\right)_{\text{c.m.}}$ (mb/sr)
5.4	210 ± 23
6.85	180 ± 19
8.0	145 ± 16
9.5	124 ± 13
11.0	106 ± 13
12.3	94 ± 0.10
13.7	71 ± 0.8
14.9	59 ± 6.5
16.25	47.5 ± 5.2
17.7	38 ± 4.1
19.2	26.4 ± 2.7
20.65	18.0 ± 1.9
23.2	9.8 ± 1.1
25.65	3.8 ± 0.5
26.9	2.28 ± 0.23
28.25	1.43 ± 0.15
31.0	0.68 ± 0.08
32.5	0.35 ± 0.04
33.85	0.25 ± 0.04
35.2	0.19 ± 0.06
36.4	0.17 ± 0.03
37.7	0.25 ± 0.025
39.1	0.25 ± 0.025
40.4	0.35 ± 0.030
41.9	0.28 ± 0.03
43.0	0.28 ± 0.03
45.6	0.23 ± 0.04
48.2	0.19 ± 0.02
50.8	0.15 ± 0.02
52.1	0.12 ± 0.012
53.3	0.086 ± 0.006
55.8	0.064 ± 0.004
58.2	0.056 ± 0.006
60.8	0.035 ± 0.007
63.25	0.022 ± 0.005
65.7	0.014 ± 0.004
71.8	0.009 ± 0.003
77.9	0.0095 ± 0.005

concluded that the contribution was less than 10% if the appropriate amount of absorber were placed in the ^3He recoil telescope.

$p\text{-}^4\text{He}$

The $p\text{-}^4\text{He}$ cross section and polarization were measured with the seven-element range telescopes only. For the polarization two symmetrically positioned matched range telescopes, simultaneously recorded protons scattered left and right from the liquid-helium target. Asymmetries were measured for protons which stopped in the various range increments between counters (3, 4); (4, 5); (5, 6); (6, 7). The telescope absorbers were adjusted so that the mean range of the scattered proton occurred at detector 4. Consistent and equal asymmetries within statistics were obtained for the range increments (5, 6) and (6, 7). These were used to calculate the polarization. Increments (3, 4) and (4, 5) showed variations and were assumed to be contaminated by inelastic scattering because the energy spread of the incident beam (30 MeV FWHM) was greater than the breakup threshold for ^4He .

DATA REDUCTION

A. Differential Cross Section (by Range Method)

The differential cross section was computed from the following formula:

$$\frac{d\sigma}{d\Omega} = \frac{N}{\phi G(\theta)\epsilon\rho}, \quad (1)$$

TABLE VII. $p\text{-}^4\text{He}$ polarization at 540 MeV.

Proton center-of-mass scattering angle, $\theta_{p,c.m.}$ (deg)	Polarization and error, $P \pm \Delta P$
5.4	0.286 ± 0.108
8.2	0.385 ± 0.028
10.9	0.485 ± 0.031
13.6	0.536 ± 0.015
16.4	0.475 ± 0.032
20.4	0.451 ± 0.029
23.1	0.365 ± 0.015
27.1	0.154 ± 0.040
29.8	0.049 ± 0.056
31.1	0.044 ± 0.066
33.7	-0.160 ± 0.056
36.3	0.145 ± 0.065
40.3	0.305 ± 0.078
45.5	0.483 ± 0.103
50.6	0.476 ± 0.073
55.6	0.453 ± 0.117

where

N = number of scattered protons detected,

ϵ = detector efficiency for a single detector or the product of efficiencies in the associated-particle mode,

ρ = nuclear density of the target,

ϕ = number of incident protons, proportional to the number of beam monitor counts;

$$G(\theta) = \frac{X_1 X_2 h}{R(R-l)\sin\theta} \text{ for liquid and gas targets,} \quad (2)$$

where

X_1 = width of the first detector element in the telescope,

X_2, h_2 = width and height of the second element,

R = target to second element distance,

l = distance between elements 1 and 2,

θ = the laboratory scattering angle;

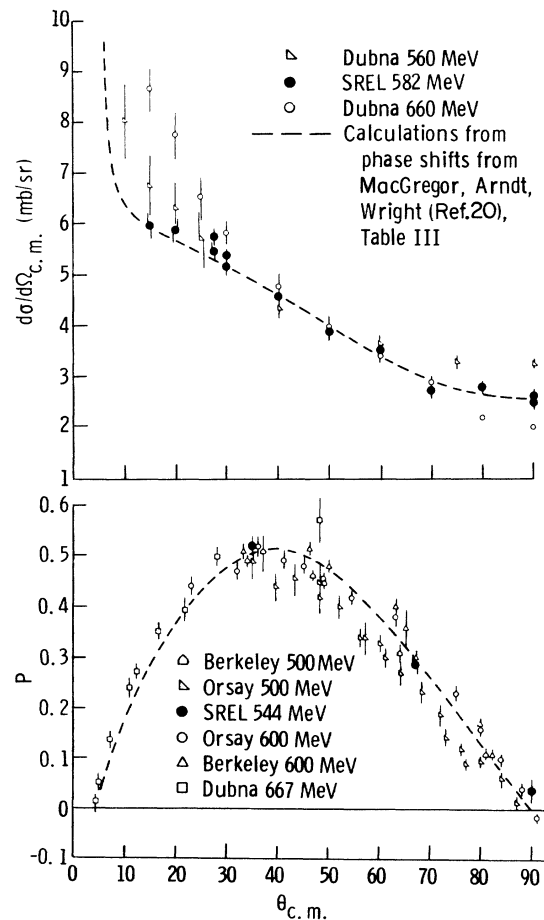


FIG. 3. Proton-proton scattering cross section and polarization.

and

$$G(\theta) = X_2 h_2 t / R^2 \cos \beta, \text{ for solid targets,}$$

where

$$t, \beta = \text{target thickness and angle.} \quad (3)$$

Absolute errors in computation of the cross sections arise from uncertainties in the incident flux and the solid-angle measurements for the detectors. Relative errors were principally due to background subtraction and uncertainties in the measurements of telescope efficiency.

B. Polarization

The asymmetry,

$$A = \frac{N_{\text{right}} - N_{\text{left}}}{N_{\text{right}} + N_{\text{left}}},$$

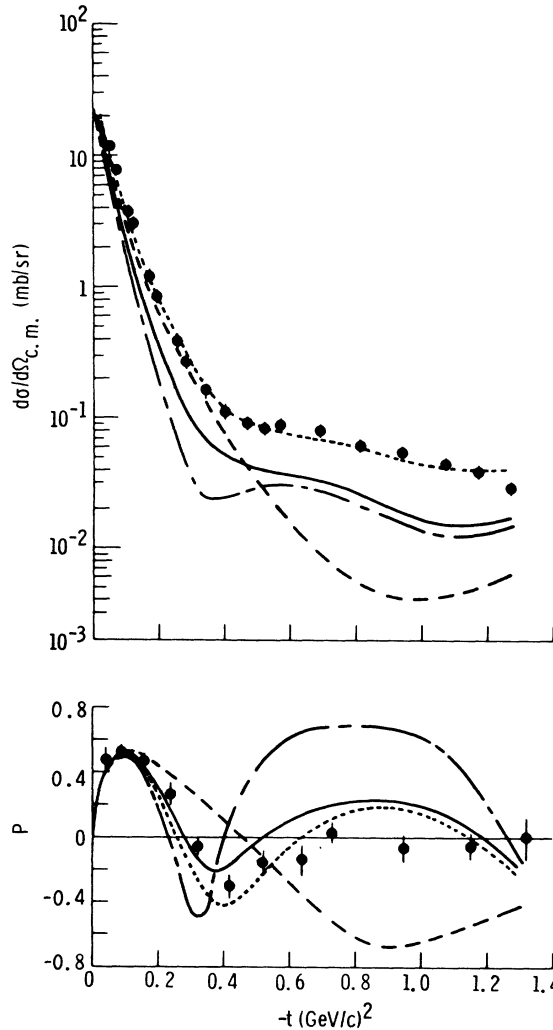


FIG. 4. Proton-deuterium elastic scattering cross section (582 MeV) and polarization (544 MeV).

observed in a coplanar double-scattering experiment is the product of polarization of the incident beam (P_1) and the polarization due to the scattering from the target (P_2):

$$A = P_1 P_2. \quad (4)$$

The asymmetries computed were the average of measurements made with detector arms in both spatially symmetric configurations.

The false asymmetry due to beam misalignment was estimated from the following:

$$\delta A = \frac{d^2\sigma}{d\Omega d\theta} \times \frac{\Delta\theta}{d\sigma/d\Omega}, \quad (5)$$

where ($d^2\sigma/d\Omega d\theta$) is the slope of the differential cross section, and $\Delta\theta$ is accumulated alignment error.

The maximum estimated value of instrumental asymmetry was ± 0.03 and ± 0.045 for the p -D and p - ^4He measurements, respectively.

RESULTS AND DISCUSSION

The experimental data obtained in this experiment are listed in Tables II to VII, and a detailed discussion of errors is contained in a laboratory note.¹⁹

p - p

There is a great deal of information in the literature on the polarization in p - p scattering near 600 MeV, but only few data on the differential cross section.²⁰ Therefore, we have measured the differential cross section between 15 and 90°, but we have taken only a few polarization data, mainly to serve as check points for our beam polarization. The results are shown in Fig. 3 in comparison with the predictions from the phase-shift solution for 570 MeV (Table III, Ref. 20) by MacGregor, Arndt, and Wright.

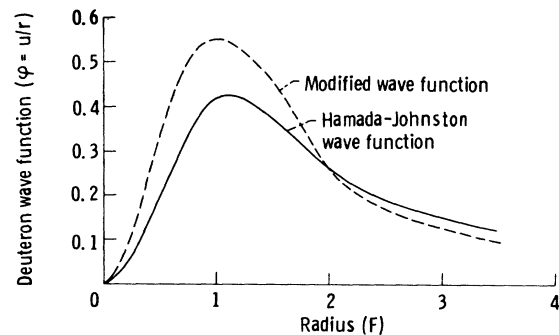


FIG. 5. Comparison of wave function obtained by Remler (Ref. 27) in fitting p -D data with the Hamada-Johnston wave function (Ref. 29).

p-D

High-energy proton-deuteron scattering cross sections have been analyzed²¹⁻²⁶ mainly in terms of the Glauber theory using spin-independent $N-N$ scattering amplitudes. Satisfactory agreement with the data has been obtained if the D -wave part of the wave function is included.

A different approach has been taken by Remler²⁷ in calculating the differential cross section and the polarization in p - D scattering at our energy. The single- and double-scattering terms in the multiple-scattering series were computed neglecting exchange terms. The problem was treated relativistically in the center-of-mass frame and the correct free nucleon-nucleon amplitudes calculated from the phase shifts. The deuteron S -state wave function was represented as the sum of three Gaussian functions and a search over the shape parameters for the best fit to the data was carried out. The D -state wave function (Table I potential 8 of Glendenning and Kramer²⁸) was renormalized to about 7% of the total wave function. The results are presented in Fig. 4. The solid, dashed, and dot-dashed lines correspond to calculations using the Hamada-Johnston wave function.²⁹ The dashed curve corresponds to single scattering only while the dot-dashed line corresponds to single and double scattering. The solid line is the result when the D state is included. The large change in the predicted polarization at larger t values obtained by including the D -state wave function may suggest a more sensitive way of determining the D -wave percentage. The dotted line in Fig. 4 is an excellent fit to the data which was obtained with a modi-

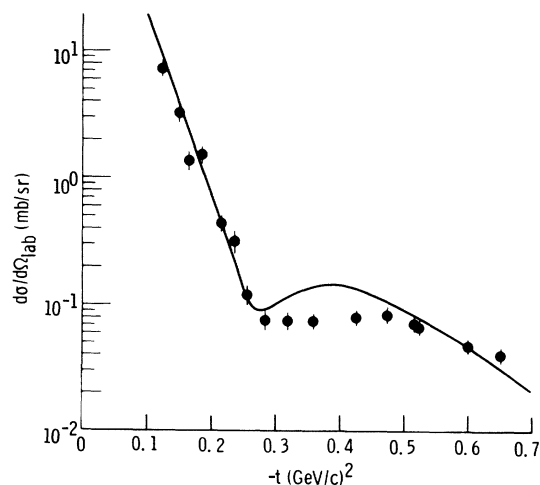


FIG. 6. Proton-helium-3 differential cross section (582 MeV). Solid line is a calculation using Glauber theory.

fied wave function as seen in Fig. 5. Its shape is quite similar to that developed by Bressel, Kerman, and Rouben³⁰ from a soft-core potential. It should be noted that the approximations used in the p - D calculations are not valid for $t > 1$ (GeV/c)², but for the region $t < 0.6$ (GeV/c)² they should be fairly accurate. Although the analysis in its present state is still inconclusive, it indicates that the data may contain new information on the deuteron structure.

Recently new data on elastic scattering and polarization⁵ and scattering from a polarized deuteron target⁴ have become available. These data, together with ours, have been analyzed using a generalized Glauber theory including spin.³¹ All of

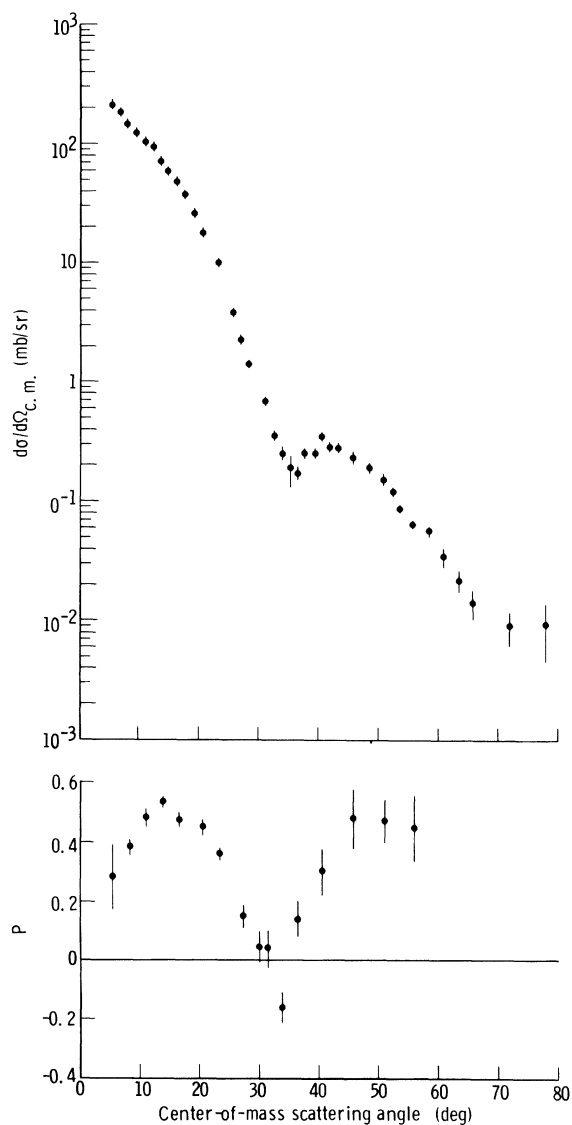


FIG. 7. Proton-helium-4 differential cross section (587 MeV) and polarization (544 MeV).

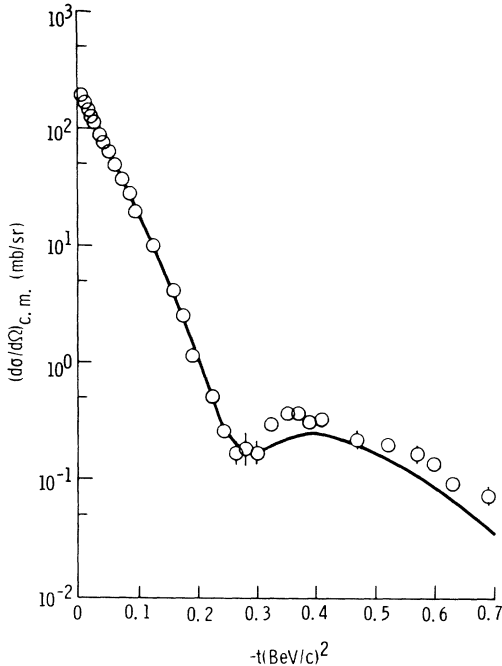


FIG. 8. Comparison of p - ${}^4\text{He}$ cross section with Glauber-theory prediction.

the p -D data are well fitted for $t < 0.25$ $(\text{GeV}/c)^2$, but rather poorly for larger t . In particular the inflection in the cross section at 0.5 $(\text{GeV}/c)^2$ is not reproduced. However, the authors³¹ have suggested the interesting possibility that p -D data might be used to determine the absolute phase of the nucleon-nucleon amplitudes. In fact, they have succeeded in fitting cross-section and polarization data to $t = 1$ $(\text{GeV}/c)^2$ by introducing an arbitrary phase factor to all the amplitudes.

p - ${}^3\text{He}$

In the absence of any more refined calculations we have compared our p - ${}^3\text{He}$ differential cross section with the results of the Glauber formalism in its simplest form as was first applied to ${}^4\text{He}$ by Czyz and Lesniak.³² We have taken a parametrized form for the spin- and isospin-independent N - N scattering amplitude which fits the p - p and n - p cross sections at our energy reasonably well:

$$f(k, q) = \frac{i + \alpha}{4\pi} k \sigma_T e^{-\alpha q^2/2},$$

where q is the four-momentum transfer and the variables α , σ_T , and a were taken to be 0.43, 3.9

fm^2 ,³³ and 4.3 $(\text{GeV}/c)^{-2}$, respectively. We have assumed the ${}^3\text{He}$ wave function to be the product of Gaussian single-particle wave functions neglecting states of higher angular momentum:

$$|\Psi\rangle = \rho_0 \prod_{j=1}^3 e^{-r_j^2/R^2},$$

where R is the rms radius of the nucleon centers in the system, where

$$\sum_{j=1}^3 \bar{r}_j = 0.$$

The best agreement with the forward slope of the cross section was obtained with $R = 1.50$ fm (Fig. 6). Considering the average radius of the nucleon to be 0.70 fm this would yield a ${}^3\text{He}$ matter radius of $[1.5^2 + (0.7)^2]^{1/2} = 1.71$ fm. This is about 10% smaller than the charge radius obtained from electron scattering.^{34, 35}

p - ${}^4\text{He}$

In Fig. 7 the p - ${}^4\text{He}$ differential cross section and polarization are shown. We have calculated the cross section using the same formalism as for ${}^3\text{He}$, but using a radius of 1.25 fm (Fig. 8). Reasonable agreement with the data can be obtained for $t \leq 0.25$ $(\text{GeV}/c)^2$; for larger t values there is a substantial discrepancy. At 1 -GeV incident proton energy, similar disagreement for p - ${}^4\text{He}$ scattering data has been studied in detail by Czyz and Lesniak³² and Bassel and Wilkin³⁶ both of whom tried to extract information about short-range nucleon correlations. Recently, the same data have been analyzed¹⁰ using the multiple-scattering theory of Ref. 8. Very good agreement was obtained, the biggest uncertainty being knowledge of the N - N amplitudes. There have also been Glauber-type calculations at 160 MeV and at our energy including the spin dependence in the N - N scattering amplitude in a simplified form.²⁶ A region of a very large negative polarization is predicted which is nearly independent of energy. The cross section and polarization have also been calculated at our energy by Ford and Pentz³⁷ who used the Watson multiple-scattering expansion to second order with an approximate double-scattering term. Qualitative features of the data are reproduced, although there is no detailed agreement. Similar results have been obtained by Kujawski³⁸ using an optical potential model. More detailed calculations will be necessary to understand the in detail interference between various multiple-scattering terms.

*Present address: Institut für Experimentelle Kernphysik, Universität Karlsruhe, Karlsruhe, Germany.

†Work supported in part by National Aeronautics and Space Administration Grant No. NGL-47-003-044.

‡Present address: Physics Department, Oregon State University, Corvallis, Oregon.

¹H. Palevsky, J. L. Friedes, R. J. Sutter, G. W. Bennett, G. J. Igo, W. D. Simpson, G. C. Phillips, D. M. Corley, N. S. Wall, R. L. Stearns, and B. Gottschalk, *Phys. Rev. Letters* **18**, 1200 (1967).

²G. W. Bennett, J. L. Friedes, H. Palevsky, R. J. Sutter, G. J. Igo, W. D. Simpson, G. C. Phillips, R. L. Stearns, and D. M. Corley, *Phys. Rev. Letters* **19**, 387 (1967).

³*High Energy Physics and Nuclear Structure*, edited by S. Devons (Plenum, New York, 1970).

⁴M. G. Albrow, M. Borghini, B. Bosnjakovic, F. C. Erne, Y. Kimura, J. P. Lagnaux, J. C. Sens, and F. Udo, *Phys. Letters* **35B**, 247 (1971).

⁵N. E. Booth, C. Dolnick, R. J. Esterling, J. Parry, J. Scheid, and D. Sherden, *Phys. Rev. D* **4**, 1261 (1971).

⁶R. J. Glauber, in *Lectures in Theoretical Physics*, edited by W. E. Britten *et al.* (Interscience, New York, 1959), Vol. 1, p. 315.

⁷M. L. Goldberger and K. M. Watson, *Collision Theory*, (Wiley, New York, 1964).

⁸A. K. Kerman, H. McManus, and R. M. Thaler, *Ann. Phys. (N.Y.)* **8**, 551 (1959).

⁹K. Bjornenak, J. Finjord, P. Osland, and A. Reitan, *Nucl. Phys.* **B22**, 179 (1970).

¹⁰C. Schmit, *Letters Nuovo Cimento* **4**, 454 (1970).

¹¹C. Wilkin, *Letters Nuovo Cimento* **4**, 497 (1970).

¹²O. Kofoed-Hansen and C. Wilkin, *Ann. Phys. (N.Y.)* **63**, 309 (1971).

¹³H. Feshbach, A. Gal, and J. Hufner, *Ann. Phys. (N.Y.)* **66**, 20 (1971).

¹⁴J. B. Cumming, J. Hudis, A. M. Poskanzer, and S. Kaufman, *Phys. Rev.* **128**, 2392 (1962).

¹⁵D. Cheng, B. MacDonald, J. A. Holland, and P. M. Ogdén, *Phys. Rev.* **163**, 1470 (1967).

¹⁶L. S. Azhgirei, Yu. P. Kumekin, M. G. Meshcheryakov, S. B. Nurushev, V. L. Solovyanov, and G. D. Stolevov, *Yadern. Fiz.* **2**, 892 (1965) [transl.: *Soviet J. Nucl. Phys.* **2**, 636 (1966)].

¹⁷J. F. Janni, Air Force Weapons Laboratory Report

No. AFWL-TR-65-150, 1966 (unpublished).

¹⁸The authors are indebted to Dr. H. Palevsky and R. Gibbs for their assistance in this matter.

¹⁹W. K. Roberts, J. S. Vincent, E. T. Boschitz, K. Goto, M. Blecher, P. Gugelot, C. F. Perdrisat, L. W. Swenson, and J. R. Priest, NASA Report No. TN D-5961, 1971 (unpublished).

²⁰M. H. MacGregor, R. A. Arndt, and R. M. Wright, *Phys. Rev.* **169**, 1149 (1968).

²¹V. Franco and R. J. Glauber, *Phys. Rev. Letters* **22**, 370 (1969).

²²E. Coleman and T. G. Rhoades, University of Minnesota Report No. AEC COO 1764-19, 1968 (unpublished).

²³D. R. Harrington, *Phys. Letters* **29B**, 188 (1969).

²⁴W. Czyz and L. Lesniak, *Bull. Pol. Acad. Sci.* (1967).

²⁵V. Franco, *Phys. Rev. Letters* **21**, 1360 (1968).

²⁶E. Kujawski, D. Sachs, and J. Trefil, *Phys. Rev. Letters* **21**, 583 (1968).

²⁷E. A. Remler, William and Mary Report No. WM-16, 1969 (unpublished); *High Energy Physics and Nuclear Structure* (Plenum, N. Y., 1970), p. 324.

²⁸N. K. Glendenning and G. Kramer, *Phys. Rev.* **126**, 2159 (1962).

²⁹T. Hamada and I. D. Johnston, *Nucl. Phys.* **34**, 382 (1962).

³⁰C. N. Bressel, A. K. Kerman, and B. Rouben, *Nucl. Phys.* **A124**, 624 (1969).

³¹G. Alberi, L. Bertocchi, and M. A. Gregorio, International Centre for Theoretical Physics, Trieste Report No. IC/71/147, 1971 (unpublished).

³²W. Czyz and L. Lesniak, *Phys. Letters* **24B**, 227 (1967).

³³D. V. Bugg, D. C. Salter, G. H. Stafford, R. F. George, K. F. Riley, and R. J. Trapper, *Phys. Rev.* **146**, 980 (1966).

³⁴R. Hofstadter, in *Electron Scattering and Nuclear and Nucleon Structure*, edited by R. Hofstadter (Benjamin, New York, 1963), p. 315.

³⁵J. S. McCarthy, I. Sick, R. R. Whitney, and M. R. Yearian, *Phys. Rev. Letters* **25**, 884 (1970).

³⁶R. H. Bassel and C. Wilkin, *Phys. Rev. Letters* **18**, 871 (1967); and *Phys. Rev.* **174**, 1179 (1968).

³⁷W. F. Ford and N. E. Pentz, NASA Report No. TM X-52594, 1969 (unpublished).

³⁸E. Kujawski, *Phys. Rev. C* **1**, 1651 (1970).